

# Simulation of high power with low threshold current of violet InGaN laser diode based on optimization of its active region

RAFID A. ABDULLAH\*, KAMARULAZIZI IBRAHIM

*Nano-Optoelectronics Research and Technology Laboratory (N.O.R), School of Physics, Universiti Sains Malaysia, 11800 Penang, Malaysia*

The simulation of high power with low threshold current of violet InGaN laser diode (LD) based on optimization of its active region has numerically been investigated. The simulation results indicated that the active region plays an important role for optimization of violet InGaN LD. The output power as high as 128 mW has been obtained, while the threshold current is 13 mA, corresponding threshold current density  $1.73 \text{ kA/cm}^2$  is observed, the threshold voltage is 4 V. The importance of this simulation study of the violet InGaN LD is the coupling between relatively higher power with lower threshold current density.

(Received February 05, 2010; accepted March 12, 2010)

*Keyword:* Violet laser diode, Quantum well laser, InGaN

## 1. Introduction

III-V nitrides compound semiconductors have attracted much attention because of their large direct band gap which is appropriate for short-wavelength LEDs and LDs [1]. The violet LDs with short emission wavelength, especially, approximately (405 nm) have attracted great interest as a light source for extra-large capacity or high-definition digital versatile disc system (DVD) [2, 3].

The active region of the LDs consists of multi-quantum-wells (MQWs), and the MQWs consist of the QWs and barriers; laser takes place in the QWs. By controlling the thickness of QWs, electron and hole wavefunctions can be modified. This results in the improvement of laser characteristics, as well as the introduction of new semiconductor optical devices [4]. The main purpose of the barrier layers in the MQWs active region of the LDs is preventing coupling between adjacent wells.

The inherent built-in polarization in c-plane GaN-based alloys is one of most important properties which limit the development of GaN-based optoelectronic devices [4]. The built-in polarization includes piezoelectric and spontaneous polarization. The piezoelectric polarization is formed when materials with different lattice constants come together which, in turn, leads to QCSE [5]. The QCSE creates band bending in the QWs; making the electrons move to one side, while the holes move to the other side of the QW [6]. This QCSE red shifts the spectral lines. On the other hand, spontaneous polarization exists due to the electrical field in the intrinsic material which leads to forming a second QCSE which blue shifts the spectral lines. The net effect of these two kinds of QCSE is the sum of their effects. Since the blue shifting effect is affected by forward biasing, a blue shift with increasing injection current is expected to be observed [7]. This

polarization has potential effects on the properties of the blue-violet InGaN-based LDS. By optimization of the active region of the LDs this effect can be reduced.

In this paper, the performance of the violet InGaN LD based on optimization of the thicknesses of QWs and barriers in the active region has numerically been investigated by using **ISE TCAD** (Integrated System Engineering Technology Computer Aided Design) software simulation program.

## 2. Laser diode structure and parameters

The two-dimensional ISE TCAD simulation program is utilized. Carrier drift-diffusion model and Newton method are used. The ISE TCAD self-consistently solves electronic and optical equations in a quantum well laser. The carrier capture model in the quantum well is linked to the electronics and optic equations. Auger and Shockley-Read-Hall (SRH) non-radiative recombination deplete the QW carriers [5]. The electronic equations are the Poisson and the continuity equations of both free and bound electrons and holes. A scalar Helmholtz equation is used to solve the optical problem, and a photon rate equation is used to calculate the photon spectrum of each mode where the photon rate equation contains the model gain, the optical loss, and the spontaneous emission. The total optical losses are: free carrier absorption loss, cavity loss, background optical loss, and waveguide loss [5]. The electronic band structure of quantum well is calculated using k.p theory of wurtzite semiconductors [6]. Spontaneous and stimulated optical recombinations are calculated in the active region according to Fermi's golden rule. As a result, the coupling between the optical and electronic equations leads to convergent problems of the Newton method [5].

A schematic diagram of the violet InGaN laser diode structure under study is shown in Fig. 1. In this simulation, it is assumed that the InGaN laser diode is grown on the n-type GaN layer whose thickness is 2  $\mu\text{m}$ . On the top of this GaN layer is a 0.1-  $\mu\text{m}$ -thick n-type  $\text{In}_{0.05}\text{Ga}_{0.95}\text{N}$  compliance layer and a 0.48-  $\mu\text{m}$ -thick n-type  $\text{Al}_{0.07}\text{Ga}_{0.93}\text{N}$  cladding layer, followed by a 0.1- $\mu\text{m}$ -thick n-type GaN guiding layer. The active region of the preliminary laser diode under study consists of double  $\text{In}_{0.12}\text{Ga}_{0.88}\text{N}$  undoped quantum wells where the thickness of every well is 2.5 nm, and every well is sandwiched between two 5-nm-thick  $\text{In}_{0.01}\text{Ga}_{0.99}\text{N}$  barriers. A 0.02- $\mu\text{m}$ -thick p-type  $\text{Al}_{0.2}\text{Ga}_{1-0.8}\text{N}$  blocking layer is grown on top of the active region, followed by a 0.1- $\mu\text{m}$ -thick p-type GaN guiding layer and a 0.48- $\mu\text{m}$ -thick p-type  $\text{Al}_{0.07}\text{Ga}_{0.93}\text{N}$  cladding layer. Finally, a 0.1- $\mu\text{m}$ -thick p-type GaN cap layer is grown over p-type cladding layer to complete the structure. The doping concentrations of n-type and p-type are equal to  $5 \times 10^{18} \text{cm}^{-3}$  and  $1 \times 10^{18} \text{cm}^{-3}$  respectively. The active region is 1  $\mu\text{m}$  in width and 750  $\mu\text{m}$  in length. The reflectivities of the two end facets are 50% for each one.

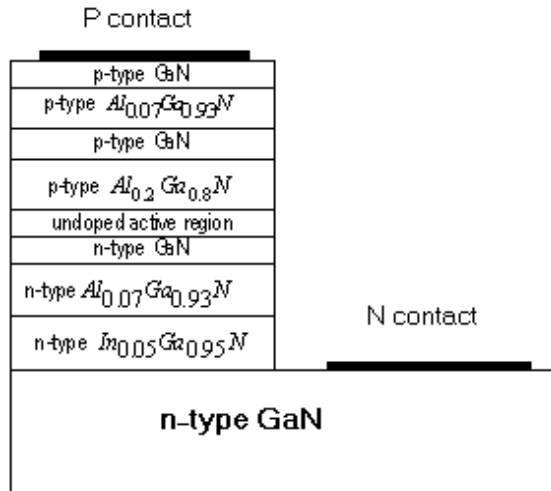


Fig.1. The schematic diagram of violet InGaN laser diode under study.

The parameters required for the k.p. method calculations of the AlInGaN materials can be obtained by a linear interpolation between the parameters of the relevant binary semiconductors (Table 1). For physical parameter  $P$ , the interpolation formula is [7]:

$$P(\text{Al}_x\text{In}_y\text{Ga}_{1-x-y}\text{N}) = P(\text{AlN})x + P(\text{InN})y + P(\text{GaN})(1 - x - y) \quad (1)$$

It is evident that, when  $x = 0$  in formula (4), the formula becomes for InGaN alloy, also when  $y = 0$ , the formula becomes for AlGaN alloy.

Table 1. Binary semiconductor parameters [8,9,10].

Parameter	symbol (unit)	GaN	AlN	InN
Lattice constant	$a_o$ ( $\text{\AA}$ )	3.189	3.112	3.545
Spin-orbit split energy	$\Delta_{so}$ ( $\text{\AA}$ )	0.017	0.019	0.005
Bandgap energy	$E_g$ (eV)	3.42	6.2	0.77
Elastic stiffness constant	$C_{33}$ (GPa)	398	373	224
Elastic stiffness constant	$C_{13}$ (GPa)	106	108	92
Electron effective mass	$m_e$ ( $m_o$ )	0.2	0.4	0.11
Heavy hole effective mass	$m_{hh}$ ( $m_o$ )	1.595	3.53	1.44
Light hole effective mass	$m_{lh}$ ( $m_o$ )	0.26	3.53	0.157

### 3. Simulation results and discussion

Fig. 2 shows the energy bandgap diagram of LD under study. The right side of the diagram is assumed to be n-side and the left side of the diagram is assumed to be p-side of the laser structure. The horizontal axis which is entitled vertical position is assumed to be the distance along the crystal growth direction.

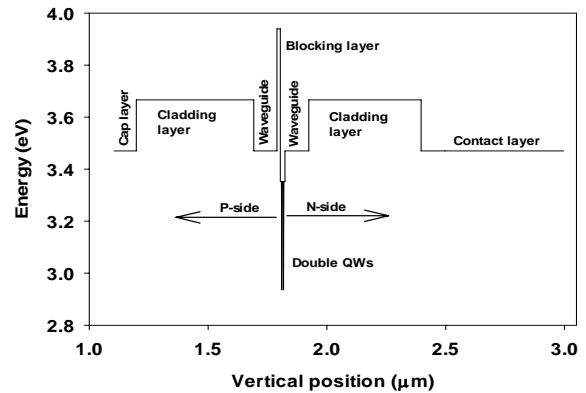


Fig. 2. The energy bandgap diagram of LD.

The band diagrams of QWs become tilted due to quantum confined stark effect (QCSE). These tilted bands will cause the special separation of electrons and holes and result in the decrease of stimulated recombination rate because the probability of electron-hole recombination is reduced. Fig. 3 shows the energy band diagrams of LD under study. The built-in polarization leads to strong deformation of the normal rectangular QW. Hence, the LDs performance could be deteriorated due to the decrease of overlapping between the electron and hole wavefunctions.

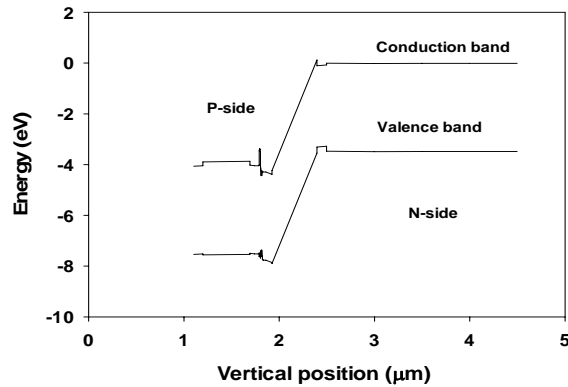


Fig. 3. The conduction and valence energy bands of LD.

Fig. 4 shows the threshold current and output power of the LD as a function of QW thickness. As it can be seen, the threshold current is strongly dependent on the QW thickness due to QCSE, and output power reduces with increasing QW thickness due to increase the threading dislocation. The reducing of the output power with increasing threshold current when the well is thinner than 2.5 nm is attributed to an increase in the nonradiative recombination on the heterointerfaces. As it is indicated from Fig. 4, the best thickness of the QW is 2.5 nm.

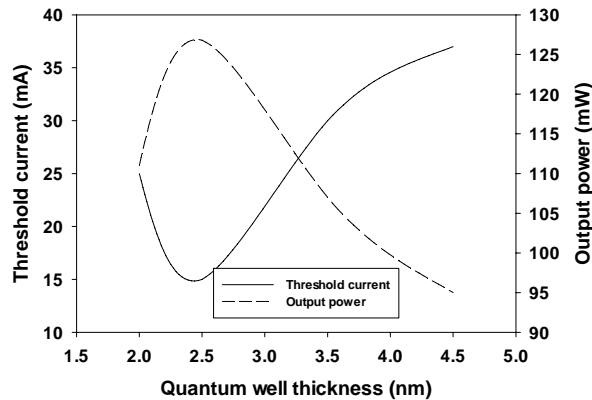


Fig. 4. Threshold current and output power versus QW thickness.

To find the best thickness of the barrier layer, the barrier thickness is varying, while keeping the thickness of the QWs constant at the 2.5 nm. The increase in the barrier thickness makes the interfaces in the MQWs rougher. This can be attributed to the deterioration of the interfacial structure quality of the MQWs caused by the generation of the defect such as threading dislocation through the partial relaxation of the strain accumulated in the MQWs [11]. Therefore, the radiative recombination process inside the QW is limited, while the non-radiative recombination increases as heat inside the structure [12]. As a results, the output power decreases; while the threshold current

increases when the barrier thickness is larger, as indicated in Fig. 5. Fig. 5 is also indicated the best thickness of the barrier is 4 nm.

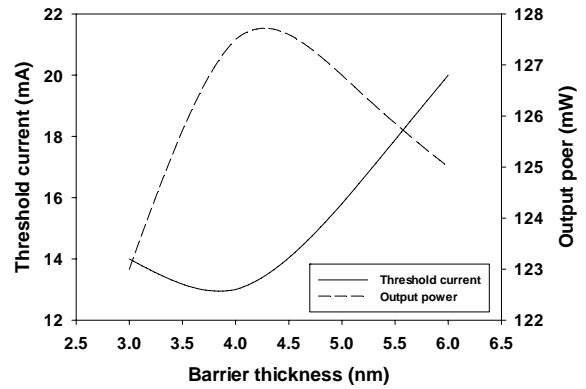


Fig. 5. Output power and threshold current versus barrier thickness.

Since the main purpose of the barrier layers in the MQWs active region of the LDs is preventing coupling between adjacent wells, hence, when the thicknesses of the barriers are thin enough, the wavefunctions of electrons and holes would penetrate the adjacent well layer, resulting in the interwell transitions. This leads to increase the piezoelectric field [13] which in turn increases the threshold current and reduce the output power of the LD.

The I-L-V curve characteristics of the LD whose QWs and barriers thicknesses are 2.5 nm and 4 nm are shown in Fig. 6. A 13 mA threshold current is obtained, corresponding to the threshold current density of 2 kA/cm<sup>2</sup>. The LD has a threshold voltage of 4 V, a maximum output power of 128 mW and lased at room temperature (300 K).

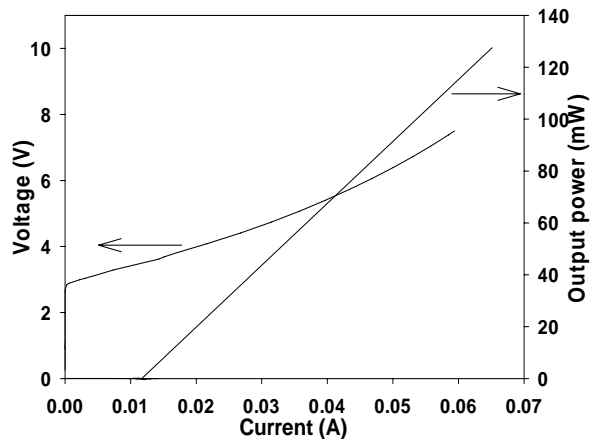


Fig. 6. The characteristic of LD with barrier thickness of 4 nm.

The vertical profile of refractive index and optical intensity of the LD with 2.5 nm-QW thickness is shown in Fig. 7. As expected, most of the optical intensity is restricted inside the active region due to the optical

confinement supplied by the GaN waveguide and AlGaIn cladding layers.

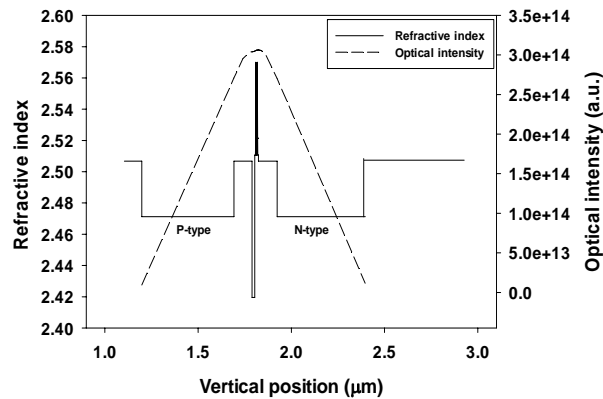


Fig. 7. The vertical profile of refractive index and optical intensity of the LD with 2.5 nm-QW thickness and 5 nm-barrier thickness.

#### 4. Conclusions

The active region has potential effects on the properties of violet InGaIn LD. Simulation results indicated that high output power with low threshold current can be obtained by optimizing the thicknesses of QWs and barriers in the MQWs active region. The best thicknesses of QWs and barriers in the active region are 2.5 nm and 4 nm, respectively for violet InGaIn-based LDs.

#### References

- [1] S. Nakamura, G. Fasol, *The Blue Laser Diode*, Berlin, Germany, Springer-Verlag, 1997.
- [2] S. Nakamura, InGaIn-based violet laser diodes, *semicond. Sci. Technol.* **14**, R27-R40, 1999.
- [3] T. Asano, M. Takeya, T. Mizuno, S. Ikeda, Y. Ohfuji, T. Fujimoto, K. Oikawa, S. Goto, T. Hashizu, K. Aga, M. Ikeda, *Proc. SPIE*, **5365**, 297 (2004).
- [4] Y. Arakawa, A. Yariv, *IEEE J. Quantum Electron.* **22**, 1887 (1986).
- [5] ISE TCAD user's manual release 10.0, Zurich, Switzerland, 2004.
- [6] S. L. Chuang, C. S. Chang, *Phys. Rev. B* **54**, 2491 (1996).
- [7] J. Minch, S. H. Park, T. Keating, S. L. Chuang, *IEEE J. Quantum Electron.* **35**, 771 (1999).
- [8] V. Fiorentini, F. Bernardini, O. Ambacher, *Appl. Phys. Lett.* **80**, 1204 (2002).
- [9] D. Fritsch, H. Schmidt, M. Grundmann, *Phys. Rev. B* **67**, 235205 (2003).
- [10] Michael E. Levinshtein, Sergey L. Rumyantsev, Michael S. Shur, *Properties of Advanced Semiconductor Materials*, John Wiley & Sons, Toronto, Canada, 2001.
- [11] Dong-Joon Kim, Yong-Tae Moon, Keun-Man Song, Seong-Ju Park, *Jap. J. Appl. Phys.* **40**, 3085 (2000).
- [12] S. M. Thahab, H. Abu Hassan, Z. Hassan, *Opt. Express* **15**, 2380 (2007).
- [13] Yong-Hoon Cho, J. J. Song, S. Keller, M. S. Minsky, E. Hu, U. K. Mishra, S. P. DenBaars, *Appl. Phys. Lett.* **73**, 1128 (1998).

\*Corresponding author: rafid\_alabdali@yahoo.com